T_c suppression and conduction mechanisms in $Bi_{2.1}Sr_{1.93}Ca_{0.97-x}R_xCu_2O_{8+y}$ (R = Pr, Gd, and Er) systems

P. Sumana Prabhu, M. S. Ramachandra Rao, and U. V. Varadaraju
Materials Science Research Centre, Indian Institute of Technology, Madras 600 036, India

G. V. Subba Rao
Central Electrochemical Research Institute, Karaikudi 623 006, India

(Received 10 February 1994)

Systematic substitutional studies in the $Bi_{2.1}Sr_{1.93}Ca_{0.97-x}R_xCu_2O_{8+y}$ (R = Pr, Gd, Er; $0 \le x \le 0.3$ in steps of 0.05 and $0.4 \le x \le 0.97$ in steps of 0.1) system were carried out in order to determine the effect of the magnetic moment and ionic radius of the rare-earth ion on the T_c suppression rate. X-ray-diffraction studies indicate that the solid solubility of Gd and Er exists up to $x = 0.97$ whereas that of Pr is limited to $x = 0.6$ under the preparative conditions employed. Resistivity and ac susceptibility studies have shown that superconductivity persists up to $x = 0.4$ and a metal-semiconductor transition occurs for $x > 0.4$. The most interesting observation is that the rate of T_c suppression for the superconducting phases is found to be identical for all rare earths. We have explained that hole filling rather than Abrikosov-Gor'kov pair breaking is responsible for the decrease in T_c. The insulating phases with $0.5 \le x \le 0.97$ exhibit the phenomenon of Mott's variable-range-hopping mechanism (VRH). The physical parameters related to VRH such as localization length (α^{-1}), hopping range (R), and activation energy (W) for conduction, have been evaluated and discussed in detail.

INTRODUCTION

The most striking feature of the high T_c superconducting oxide materials is the existence of a parent compound which is insulating viz., La_2CuO_4, $YBa_2Cu_3O_6$, Nd_2CuO_4 etc. Upon adequate doping these materials can be driven from a Mott-Hubbard insulating regime to the metallic regime and at optimum doping concentrations superconductivity is encountered. Thus, by adopting proper preparative conditions and by choosing appropriate substituents, a variety of metallic (superconducting) and semiconducting phases can be synthesized that exhibit remarkable physical properties. While the superconducting phase in the $RBa_2Cu_3O_7$ (R = rare earth) system has noninteracting magnetic moments irrespective of the nature of the rare-earth (RE) ion, the corresponding insulating phase ($RBa_2Cu_3O_6$) is an antiferromagnetic insulator. The only exception is $PrBa_2Cu_3O_7$ which is an insulator. The insulating behavior is attributed to the interaction of the Pr magnetic moments with the Cu3d-O2p band. In the $(Y_{1-x}Pr_x)Ba_2Cu_3O_7$ system, the T_c decreases drastically with increase in Pr content and the trend of T_c suppression as a function of x is very consistent with the phenomenon of Abrikosov-Gor'kov (AG) pair breaking mechanism.[1]

Insulating phases in the $Bi_2Sr_2CaCu_2O_{8+y}$ (Bi-2212) have also been identified by systematic substitutional studies at the Ca site by Y or RE ion.[2-6] As the substituent concentration increases, the system changes over to an insulator with Neèl temperature as high as 375 K when all the Ca^{2+} is replaced by Y^{3+}. Although similar substitutional studies by other rare earths (RE) at the Ca site have been made, systematic comparative studies of the rate of T_c suppression for various rare earths are very few in the literature. Moreover, the mechanism that governs the T_c suppression as well as the mechanism of conduction at higher dopant levels in such cationic disordered systems have not been reported, hitherto. It is well delineated that for the AG pair breaking theory to hold good, the T_c should decrease at a rate proportional to the magnetic moment of the impurity atom (RE ion in this case) and follow a universal trend as described by Abrikosov and Gor'kov.[7] Similarly, the trends in the decrease of the superconducting energy gap and specific heat have been well established. The interesting feature in this article is a systematic comparative study of the T_c suppression rate by Pr, Gd, and Er of varying ionic radii and magnetic moments ($\mu_{\text{eff}}^{\text{Pr}} = 3.5\mu_B$, $\mu_{\text{eff}}^{\text{Gd}} = 7.9\mu_B$, and $\mu_{\text{eff}}^{\text{Er}} = 9.6\mu_B$). This work aims at highlighting two important aspects: (i) to verify whether the trend of T_c suppression as a function of rare-earth concentration is AG-like or otherwise and (ii) to elucidate the underlying conduction processes in the non-superconducting phases by applying the well-known Mott's variable range hopping (VRH) mechanism.

The dramatic effect of Pr in $(Y_{1-x}Pr_x)Ba_2Cu_3O_7$ which is still the focal point of intense research activity and the conflicting reports regarding the nature and role on the T_c suppression rate, of Pr substitution in the Bi-2212 system, have provided incentive to study the effect of Pr at the Ca site in comparison to more magnetic Gd and Er. We report herein a detailed discussion on the validity of the AG pair breaking theory versus hole filling mechanism ($0 \le x \le 0.4$) in the superconducting phases. In addition, a detailed evaluation of various physical parameters from our experimental data on the insulating phases ($0.5 \le x \le 0.97$) is also presented that provide an

excellent insight and understanding of the VRH mechanism.

EXPERIMENT

The Bi-2212 superconducting oxide system has been extensively studied and various starting compositions of Bi:Sr:Ca:Cu have been adopted to obtain single phase materials. The $T_{c,\text{zero}}$ (superconducting transition temperature at which the resistance completely goes to zero) values reported for this phase range from 60–85 K depending on the preparative conditions and final annealing and/or quenching temperature. The $T_{c,\text{zero}}$ values depend on the Ca/Sr ratio and Bi content and also on the final heat treatments such as quenching in air/liq.N_2 (Refs. 8–11) and annealing in an Ar/N_2 atmosphere.[12,13] Although a large number of preparative methods have been suggested in the literature, repeatability of a reported preparative method with respect to achieving phase purity and consistent $T_{c,\text{zero}}$ values is difficult. Our aim, therefore, is to obtain single phase materials of Bi-2212 with consistent values of $T_{c,\text{zero}}$. This has been achieved starting with an off-stoichiometric composition $Bi_{2.1}Sr_{1.93}Ca_{0.97}Cu_2O_{8+y}$ which conforms to the general formula $Bi_2[Bi,Sr,Ca]_3Cu_2O_{8+y}$.[14] All the compositions of the system $Bi_{2.1}Sr_{1.93}(Ca_{0.97-x}R_x)Cu_2O_{8+y}$, were prepared by solid state reaction, using a modified procedure of Ono.[14] This off-stoichiometric composition was chosen, assuming that an excess Bi in the Ca and SrO planes stabilizes the Bi-2212 phase.

The preparative conditions for the undoped phase ($x=0$) were first standardized, in order to obtain phase pure materials of Bi-2212. The starting materials, Bi_2O_3 (99.999%), CuO(99.999%), $SrCO_3$ (99.999%), and $CaCO_3$ (99.98%, all Cerac, UK), were taken in the above mole ratios, ground and calcined in air at 810 °C for 16 h. The subsequent heat treatments were also carried out in air at 840 °C for 5–6 h and 875 °C for 10 h with intermediate grinding. The material was then pressed into pellets (diameter: 8 mm and 12 mm; thickness: 1–2 mm) and sintered at 870 °C for 10 h in air and furnace cooled to room temperature. In order to enhance the T_c, the samples were introduced into a preheated furnace at 805 °C for 1–2 h and then quenched in air. We observed an increase in T_c to about 74–76 K on quenching. The procedure was repeated for several batches of samples and consistent $T_{c,\text{zero}}$ values were obtained. The rare-earth doped phases were prepared using identical heating and quenching conditions as above. However, the compositions with $x>0.3$ formed single phase materials only at higher temperatures. Hence, the final heating temperature was progressively increased from 890 °C for $x=0.4$ to 930 °C for $x=0.97$ for all RE ions in $Bi_{2.1}Sr_{1.93}(Ca_{0.97-x}R_x)Cu_2O_{8+y}$. The phases were characterized by powder x-ray diffraction (XRD) using Cu-$K\alpha$ radiation. (SEIFERT, Germany, Model P3000). Resistivity measurements were carried out by the four probe Van der-Pauw method using a closed cycle He refrigerator (CTI-Cryogenics, USA: Model M22). ac susceptibility measurements in the range 300–13 K were made with a field of 0.1 Oe and frequency 300 Hz using an automated SUMITOMO (Japan) Superconducting Materials Property Measuring Equipment (Model SCR 204-T).

RESULTS AND DISCUSSION

Structure and solid solubility

The phases of the type $Bi_{2.1}Sr_{1.93}(Ca_{0.97-x}R_x)Cu_2O_{8+y}$ (R=Pr,Gd,Er; $x=0$ to 0.3 in steps of 0.05 and $x=0.4$ to 0.97 in steps of 0.1) have been presently synthesized and studied. XRD of the samples were recorded both before and after the final annealing. Under the preparative conditions employed, the upper limit of solid solubility is $x=0.6$, 0.97 and 0.97 for the Pr, Gd, and Er substituents, respectively. To check the effect of the ionic size of the rare earths on the solid solubility limit, we also prepared the La-doped phase with $x=0.7$ and the XRD data on this phase too, indicated the presence of impurity phases of Bi-2201. This indicates that the solid solubility of the lighter rare earths in the Bi-2212 system is limited. Gao *et al.*[4] have obtained complete solubility of Pr in Bi-2212 prepared by solution technique. Whereas only 50% solubility has been observed by Awana *et al.*[15]

For compositions $x \leq 0.3$, the XRD patterns of all the rare-earth doped phases remained unchanged on quenching, whereas the XRD patterns of a few compositions with $x \geq 0.4$ showed an increase in the background intensity when quenched. For uniformity, the structural data has been calculated only on the unquenched samples using the least-squares fit of the higher angle lines. XRD patterns of different compositions are given in Figs. 1(a) and 1(b). The peaks have been indexed on the basis of a tetragonal structure at low concentrations of the rare-earth dopants. At $x=0.40$ for R=Er and at $x=0.6$ for the Pr and Gd doped phases, splitting of the (200) and (020) is observed [Fig. 1(b)], indicating orthorhombic symmetry. Also, for $x=0.8$ and 0.97 of the Gd and Er phases, the most intense lines seen were that of (001) planes [Fig. 1(bii)]. As can be seen (Fig. 2), there is a slight increase in the a-lattice parameter with increasing x, while b remains almost a constant. This is as expected, since the extra electrons introduced by the dopant ions reduce the effective valence on Cu resulting in an increase in the Cu-O bond length, which is observed as an increase in the a-lattice parameter.[16,17] The c-lattice parameter, however, decreases smoothly in all the three rare-earth doped phases. The ionic sizes of Gd^{3+} (1.053 Å) and Er^{3+} (1.004 Å) being less than that of Ca^{2+} (1.12 Å) in eightfold coordination, such a decrease is expected. The ionic size of Pr^{3+} (1.126 Å), on the other hand, is almost the same as that of Ca^{2+} and contrary to expectation, a decrease in the c-lattice parameter is observed. Xue *et al.*[18] have observed that the CuO_2-Gd-CuO_2 separation is larger than that of CuO_2-Ca-CuO_2 although the ionic size of Gd^{3+} is less than Ca^{2+}. The excess positive charge on Gd^{3+} causes a repulsion between the CuO_2 layers thereby increasing the CuO_2-CuO_2 plane separation. However, with an increase in rare-earth concentration, the oxygen content increases,[16–20] and this excess oxygen is incorporated in between the Bi_2O_2 double lay-

ers. Consequently, the net positive charge and hence the repulsion between the Bi_2O_2 layers decreases causing the slab sequence, SrO-BiO-BiO-SrO (rocksalt structure) to shrink.[18] This decrease offsets the increase in the CuO_2-R-CuO_2 separation and hence the decrease in the c-lattice parameter is due to the incorporation of excess oxygen within the Bi_2O_2 layers. There have been reports[15] of the existence of Pr in the 4+ valence state, the ionic size which is less than that of Ca^{2+}. However, magnetic susceptibility studies[21] have clearly shown that the effective magnetic moment on Pr is about $3.58\mu_B$ which is close to the free ion moment of Pr^{3+}.

Electrical, magnetic and superconducting properties

Resistivity measurements were carried out on all the rare-earth doped phases with $0 \leq x \leq 0.97$. As can be seen from Fig. 3, well-defined metallic behavior and superconducting transitions are clearly seen for all the compositions $x = 0.0-0.3$ for Pr, Gd, and Er substituted Bi-2212 phases.

The normal state resistivity $\rho(T)$, measured in the range 300–100 K follows the Mattheissen's equation $\rho(T)=\rho_0+AT$ where ρ_0 is the residual resistivity which is usually very small for good metallic behavior and the slope $d\rho/dT(A)$ is the temperature coefficient of resistivity, characteristic of the material.

For the phases with $x \leq 0.3$ for R=Pr, Gd, and Er, the superconducting transition temperature for the quenched phases was higher than that for the unquenched ones. But the $x=0.4$ concentration for all the rare-earth doped phases showed a semiconducting behavior at high temperatures and became metallic at low temperatures and no $T_{c,\text{zero}}$ values were seen. The background intensities as seen by XRD of the phases for $x>0.4$ increased on quenching. Therefore, the final step of quenching from 805 °C was not carried out for compositions $x>0.4$. The $T_{c,\text{zero}}$ versus x plot for the quenched samples is shown in Fig. 4. As can be seen, the T_c remains almost unchanged for x upto 0.15 and decreases rapidly thereafter. For the phases with $x<0.3$, the quenched samples showed higher

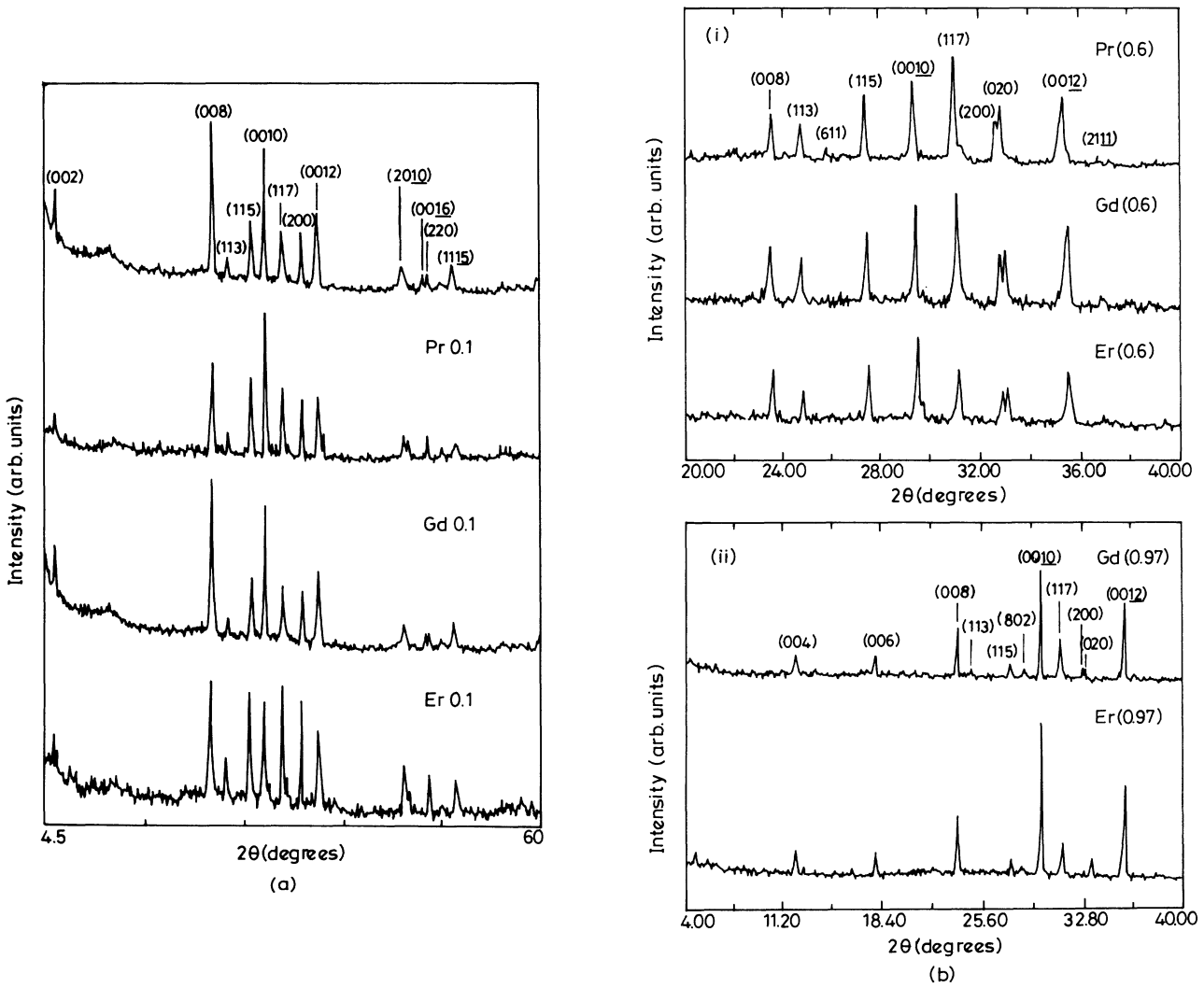

FIG. 1. (a) and (b) XRD patterns of the phases $Bi_{2.1}Sr_{1.93}(Ca_{0.97-x}R_x)Cu_2O_{8+y}$ system for various x and R=Pr, Gd, Er. Sharp (001) lines are observed in the case of the Gd and Er doped phases with $x=0.97$. For higher RE concentrations, a clear splitting of the (200) and (020) lines has been observed indicating orthorhombic symmetry.

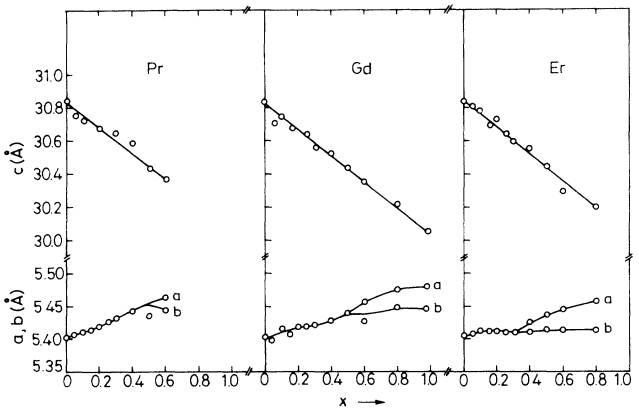

FIG. 2. Lattice constants a, b, and c for $0 \leq x \leq 0.6$ for Pr and $0 \leq x \leq 0.97$ for the Gd and Er doped phases. A change from tetragonal to orthorhombic symmetry is observed in all cases.

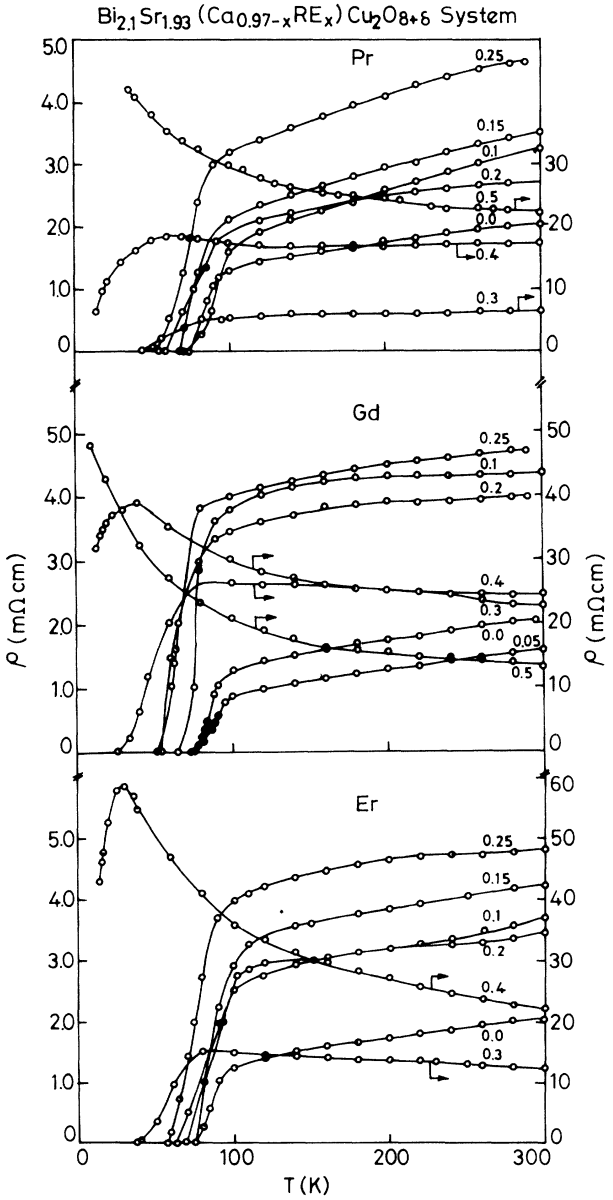

FIG. 3. Resistivity as a function of temperature for the superconducting phases. The $x=0.4$ composition shows semiconducting behavior at high temperatures for all RE.

T_c values as compared to the unquenched ones, irrespective of the rare-earth ion dopants at the Ca site. Quenching reduces the oxygen content between the BiO-double layers making it more metallic. Excess oxygen introduced in between the Bi-O double layers tends to decrease their metallicity[22] and hence the transition temperature of the materials. This was found to be true for all the three rare-earth doped compositions and is reflected in the XRD patterns also, where an increase in the background intensity is observed on quenching.

ac susceptibility measurements were carried out on all the superconducting phases at a field of 0.1 Oe and frequency of 300 Hz. The complex ac susceptibility (χ) is defined as $\chi=\chi'+\chi''$, where χ' is the in-phase (inductive) component and χ'' is the out-of-phase (resistive) component. ac susceptibility study furnishes a great deal of information regarding the superconducting transition temperature, microstructure etc.[23] All phases with

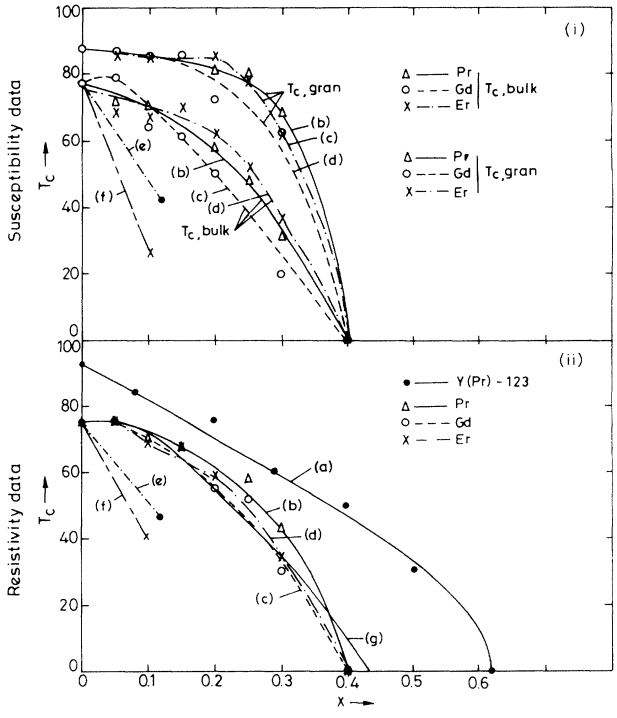

FIG. 4. (i) and (ii) The variation of T_c (from ρ-T and χ-T data) as a function of the dopant concentration ($0 \leq x \leq 0.4$). From the χ-T plots, $T_{c,\text{gran}}$ and $T_{c,\text{bulk}}$ refer to the intragranular and intergranular transitions, respectively. For comparison, the variation of T_c in the $Y_{1-x}Pr_xBa_2Cu_3O_7$ (data taken from Ref. 1) is shown (iia). The solid line is the fit to the Abrikosov Gor'kov theory. The trend in the behavior of T_c suppression in the case of Y(Pr)-123 is AG-like. Whereas in the case of RE (b, c, and d) substituted Bi-2212, it is markedly different and the decrease in T_c could be explained as due to hole filling. For comparison, the T_c vs x behavior for the Fe and Co (e and f) doped Bi-2212 phases (data taken from Ref. 24) is also shown which shows a drastic T_c suppression. Also, resistivity data (g) on the nonmagnetic Y-doped phases (data taken from Ref. 25) show similar trend as that of the magnetic rare earth substituents.

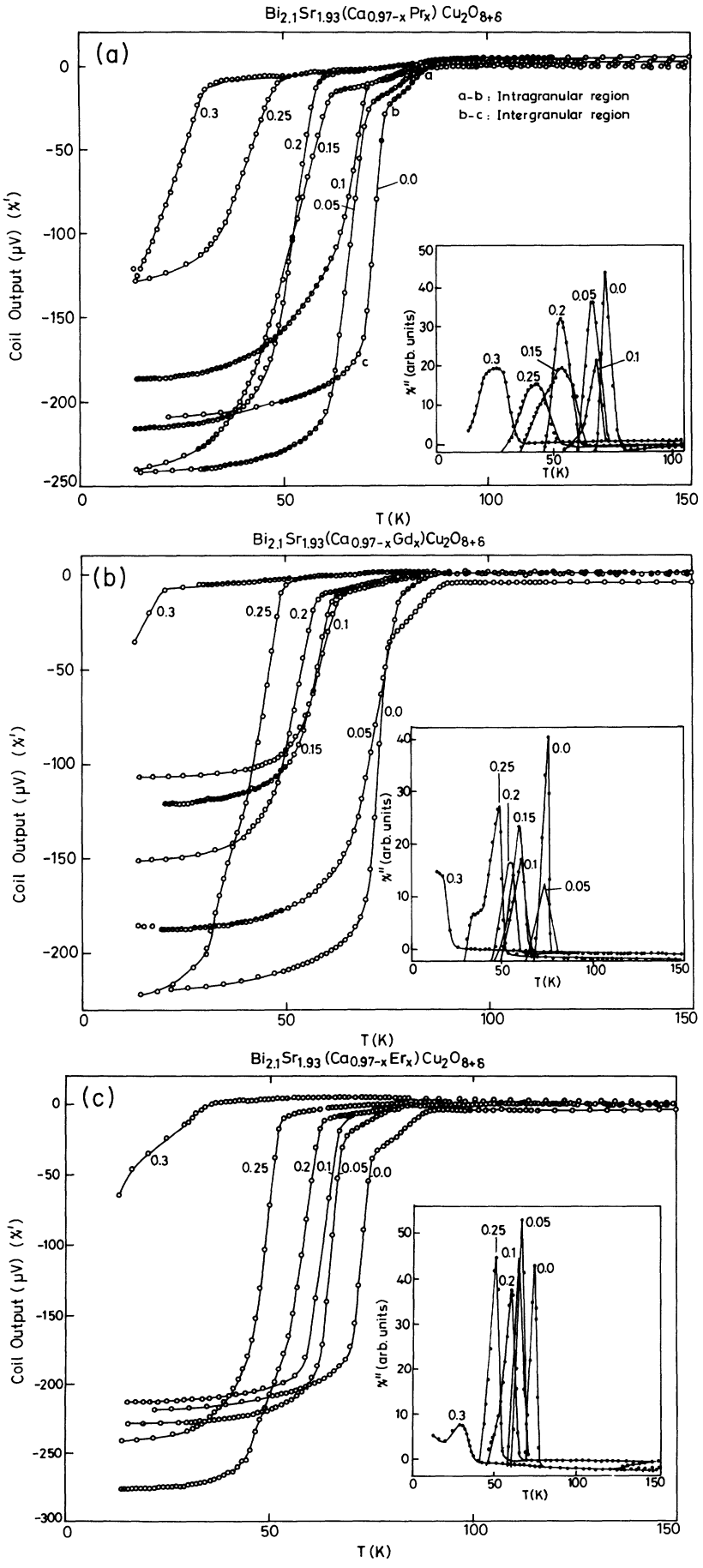

FIG. 5. Recorder traces (Sumitomo, Japan, Supercond. Mater. Prop. Meas. System) of the χ-T plots for various x in the RE doped phases-Pr (a), Gd (b), and Er (c) indicating granular and the bulk superconducting transitions. Saturation of the signal is observed for $x<0.3$. (Inset: χ''-T plots for the above phases indicating homogeneous nature of the materials). Regions marked a-b and b-c in (a) indicate intragranular ($T_{c,\mathrm{gran}}$) and intergranular ($T_{c,\mathrm{bulk}}$) contributions.

R=Pr, Gd, and Er show a Pauli paramagnetic behavior in the normal state and as the materials are further cooled to the superconducting state well-defined diamagnetic onset occurs [Figs. 5(a)–5(c)]. A sharp drop in χ' at T_c followed by a saturation of the signal at lower temperatures indicates bulk superconducting nature and excellent quality of the compounds. With increasing dopant concentration, a systematic decrease in the diamagnetic onset temperature is observed for all rare earths. For the $x=0.3$ composition the signal strength decreases and no saturation of the signal is observed down to 13 K. This may be due to the small volume fraction of superconductivity at higher concentrations. In the $\chi'-T$ curves, we refer to the high-temperature intragranular drop as $T_{c,\text{gran}}$ and low-temperature intergranular drop as $T_{c,\text{bulk}}$. When the applied magnetic field (0.1 Oe in this case) is much less than the critical field (H_{c1j}) of the weak Josephson coupling, a distinct drop occurs ($T_{c,\text{gran}}$) at higher temperatures due to the individual randomly distributed and weakly coupled grains followed by a global intergranular ($T_{c,\text{bulk}}$) drop indicative of the bulk superconducting nature of the compound. We have explained[24] that the double drop behavior is not due to any secondary phases in the compound since XRD studies clearly show the single phase nature of the phases. In addition to XRD, dc magnetization studies on select phases using a superconducting quantum interference device (SQUID) magnetometer (using fields $\sim$50 and 100 Oe) show only rounding off behavior at the onset of superconductivity due to the high fields used (discussed in Ref. 25) and a clear saturation of the signal at low temperatures. A sharp χ'' peak indicates that the material has a well-connected network of superconducting grains. Broadening of the $\chi''-T$ curve is seen for some of the phases at higher dopant levels which is due to the reduction in volume fraction of superconductivity.

AG pair breaking mechanism

It is well established that the mechanism responsible for superconductivity is the formation of bound electron (Cooper) pairs in the singlet state. The Cooper pair is a time reversal pair of a one electron state $(k\uparrow,-k\downarrow)$. Abrikosov and Gor'kov[26] (AG) have shown that the presence of magnetic impurities in a superconductor break the time reversal symmetry that causes a strong suppression of T_c and the T_c decreases at a rate proportional to the concentration (x) of the magnetic ion. The AG calculations deal with the exchange interaction between a paramagnetic impurity (of spin S) and a conduction electron (of spin s) given by $H_{\text{ex}}=-JSs$ where J is the exchange integral, a parameter characterizing the strength and sign of the exchange interaction. The rate of T_c suppression in such an interaction, would depend on the magnetic moment of the impurity ion and would be higher for the ion with a larger magnetic moment. In the BCS limit, the reduced transition temperature (T_c/T_{c0}) in the presence of such a paramagnetic impurity is given by the relation:

$$\ln(T_{c0}/T_c)=\Psi(1/2+\alpha)-\Psi(1/2)\ , \qquad (1)$$

where Ψ is the digamma function and α is the pair breaking parameter [$\alpha=1/2\pi\tau_p T_c$ for the weak-coupling BCS superconductor and $\alpha=1/2\pi\tau_p T_c(1+\lambda)$ for the strong-coupling superconductor], where $1/(1+\lambda)$ is the strong-coupling factor when $\lambda=\lambda(0)$ where λ is the coupling constant and τ_p is the life time of the carriers due to spin-flip scattering by paramagnetic impurities.[26]

A typical variation of T_c versus x is shown in Fig. 4(iia) for $(Y_{1-x}Pr_x)Ba_2Cu_3O_7$ (data reproduced from Ref. 1) which follows the universal trend of T_c variation with x as described by the AG pair breaking theory.[1,26] For small values of x, the decrease in T_c is linear with x, with a slope proportional to the magnitude of J, while at a large value of x, the decrease in T_c is more rapid. The T_c vanishes at a critical value of x ($=x_{\text{cr}}$) as shown in Fig. 4(iia).

In the present system, the T_c (from ρ-T and χ-T data) vs x plot is shown in b, c, d of Fig. 4 (i) and (ii) pertaining to Pr, Gd, and Er substitution at the Ca site (Bi-2212). Interestingly, all the three rare earths show similar trends of T_c suppression, irrespective of the magnetic moments of the dopant ions clearly indicating that the magnetic nature of the rare-earth ions do not play any role in the mechanism of T_c suppression. For the AG theory to hold good, one would expect the T_c suppression rate to vary in accordance with the magnetic moment of the impurity ions which is not at all observed in the present case. This clearly indicates that the magnetic moment of the rare-earth does not interact with the conduction electrons which may be due to the increase in the interlayer CuO_2 separation due to RE doping. The nature of T_c suppression is obviously, a clear deviation from the universal curve given by the AG pair breaking mechanism. Slight deviations in the T_c suppression rate at higher x concentrations, may be attributed to the differences in ionic radii of the respective RE ions. For comparison, the T_c vs x plot of two magnetic ions—Fe and Co at the Cu site of Bi-2212 is shown in Fig. 4(e,f) (data taken from Ref. 24). As can be seen, the T_c suppression rate is found to be very drastic even for small concentrations of the dopant ions. The end points in this case represent the solid solubility limit ($0\le x\le 0.12$) for Fe; ($0\le x\le 0.1$) for Co. From the slopes of the curves, assuming AG pair breaking mechanism, x_{cr} [calculated from ρ-T data using equation $x_{\text{cr}}(dT_c/dx)=-\pi^2 e^{-\tau}(T_{c0}/8)$, where τ is the Euler's constant $\sim$0.5772 and dT_c/dx is initial linear slope] for Fe and Co are 0.21 and 0.15, respectively. In the present case, the mechanism of T_c suppression could be due to the extra electrons introduced by the substitution of a trivalent RE ion at the Ca site which fills the Cu3d-O2p band.[27] Pr in Bi-2212 has no additional pair breaking effect in contrast to the $Y_{1-x}Pr_xBa_2Cu_3O_7$ system where the 4f electron orbital of Pr^{3+} overlaps with the CuO_2 planes causing strong localization of the mobile holes in the CuO_2 planes. Since the rate of T_c suppression of Pr in Bi-2212 is the same as that of Gd and Er, it appears that Pr exists in the 3+ valence state as has been proved in earlier studies in the literature.[20] Figure 4(iig) shows the T_c suppression in the case of nonmagnetic Y at the

Ca site (data taken from Ref. 25) which follows the same trend as that of the other three magnetic rare earths.

dc susceptibility studies[4] have shown that no ordering of Pr and Gd (for $T > 1.5$ K) in Bi-2212 is observed unlike in the case of $PrBa_2Cu_3O_7$ (Pr-123) where a clear ordering of the Pr moments ($T_N \sim 17$ K) and Gd-123 ($T_N \sim 2.25$ K) due to Gd ordering is seen. It was suggested that the coupling of the RE ions in RE doped BI-2212 is relatively different, compared to that observed in the RE substituted Ln-123 (in particular Pr-123) despite the similarities in the local environments of the ions in both the systems. The high ordering temperature of Pr in Pr-123 is due to the strong interaction of the Pr moments via Cu3*d*-O2*p* orbitals. The absence of ordering in the corresponding Bi-2212 shows that there is no such interaction. This reiterates our observation that Pr has no additional effect on the T_c suppression compared to the other rare earths.

Variable range hopping

A metal-insulator (*M-I*) transition occurs due to strong electron correlations (Mott transition) or due to some kind of disorder in the system (Anderson transition). Also, a much simpler cause viz., band filling is a distinct possibility in the present system. However, a detailed analysis of the data revealed a VRH type of behavior which rules out the above possibility. A detailed discussion is in order.

A disorder-induced transition leads to localization of states in the vicinity of the Fermi level and a finite density of states (DOS) at E_F. Conduction then takes place by the variable range hopping (VRH) mechanism[28,29] which involves hopping of carriers between the various localized states. The localized electronic states are randomly distributed in energy as well as in space, with a uniform distribution given by $N(E_F)$, which is the density of states per unit volume per unit energy. The ρ-T behavior is governed by the equation $\rho = \rho_0 \exp(T_0/T)^{1/n}$, where T_0 is the characteristic temperature and n denotes the nature of the conduction mechanism. For $n=3$ and 4, it corresponds to two-dimensional (2D) and 3D variable range hopping mechanism, respectively. The characteristic temperature T_0 is related to the electronic density of states at the Fermi level, $N(E_F)$ and "a"($=\alpha^{-1}$) is the radius of the localized states [also termed as the localization length or localization radius (ξ)] and is given by the relation

$$T_0 = 16/a^3 k N(E_F) , \quad (2)$$

where k is the Boltzmann constant. Equation (2) is representative of a three-dimensional system wherein the conduction takes place by phonon-assisted hopping between adjacent layers creating a 3D percolative path. The VRH mechanism of conduction is best described at low temperatures where the thermal energy for charge transport is insufficient to excite the carriers across the Coulomb gap. The localization length "a"($=1/\alpha$), which represents the exponential decay of the electronic wave function at large distances, can vary from a few unit cells (30–40 Å) to as small as 3–5 Å depending on the extent of disorder present in the system. In such a system, contribution to the electrical conduction is possible only by hopping (mediated by phonons) from one filled state to an empty state. Thus, the term "hopping" is related to the phonon assisted quantum mechanical tunneling of an electron from one localized state to another. Noncrystalline materials generally exhibit this phenomenon due to the absence of long-range order. Mott has experimentally verified the VRH mechanism at low temperatures in a class of systems and treatised his observations.[28,29] Such trends have been reported in the insulating phases of high T_c materials too, like the La-Sr-Cu-O system[30,31] and other rare-earth doped Bi-2212 phases.[31–33]

In the present study, the compositions with $0.5 \le x \le 0.97$ were semiconducting for the rare-earth doped phases (Fig. 6). As observed by other workers,[33,34] we found that none of the semiconducting phases ($x = 0.5$–0.97) satisfy either the thermally activated conductivity [$\ln\rho$ vs $(1/T)$] behavior or the mechanism of hopping conductivity in a system of localized electrons with long-range Coulomb interaction [$\ln\rho$ vs $(1/T)^{1/2}$]. However, they all satisfy the $n=3$(2D) and $n=4$(3D) behavior of Eq. (2). Figure 7 shows the logarithm of resistivity (ρ) as a function of $T^{-1/4}$. As can be seen, all the three rare-earth substituted phases with $x = 0.5$–0.97 satisfy the 3D VRH mechanism. The systematic increase

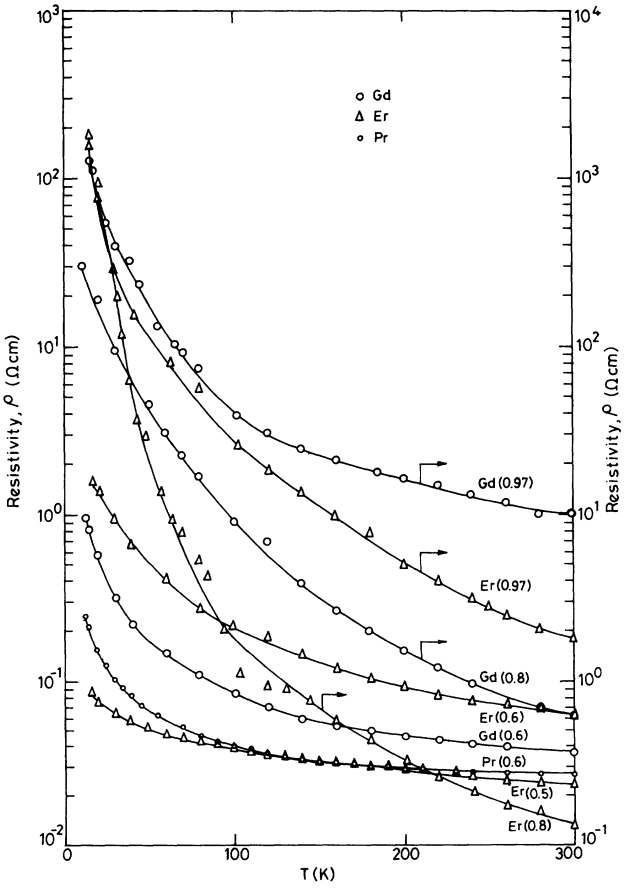

FIG. 6. Resistivity as a function of temperature for the semiconducting phases $0.5 \le x \le 0.97$ for R=Pr, Gd, and Er.

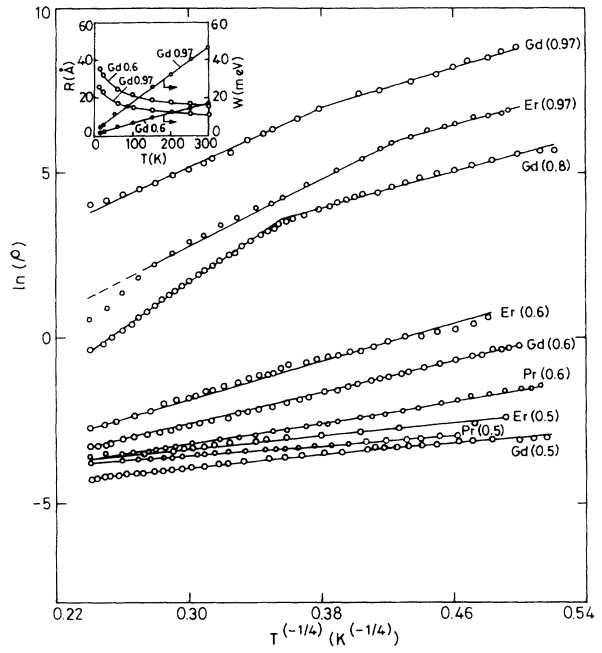

FIG. 7. $\ln\rho$ vs $T^{-1/4}$ plots for various x and R=Pr, Gd, and Er. An increase in slope observed for increasing x is an indication of the increasing disorder in the materials with increase in the dopant level. [Inset: Variation of range (R) and activation energy (W) with temperature].

in slope with increasing x implies that the material becomes more and more disordered with increase in dopant levels. The disorder tends to slow down or localize a carrier at the lattice sites resulting in the formation of polarons.[35] If the carrier is confined to a single site, it is referred to as a small polaron. For higher concentrations with x=0.8 and 0.97, a double slope behavior is observed. This may be explained as follows: Conduction normally takes place by hopping of electrons between the various available localized states in the vicinity of the Fermi level. The energy (W) for this is acquired from the phonons. This can be greater or lesser than kT depending on the concentration of dopants.[36] For x=0.5 and 0.6, $W \sim kT$, which is due to the single-phonon hopping mechanism, where the energy is sufficient for an electron to hop to the final state in a direct transition.[37] This is as expected, since at low dopant concentration (x=0.5 and 0.6), the impurity level is less (i.e., disorder is less) and hence a direct transition from the filled state to the unfilled state is feasible. At higher concentrations, (x=0.8 and 0.97), the disorder is considerably enhanced (as is also evident from the high values of $T_0 \sim 10^6$ K), in which case, conduction takes place only by an exchange transition to the final state. This involves a complex percolation network, with the electron making a transition initially to levels higher in energy than kT. The additional energy is supplied to the electron by mutliphonon pro-

TABLE I. Calculated parameters of the semiconducting phases ($0.5 \le x \le 0.97$) in the $Bi_{2.1}Sr_{1.93}Ca_{0.97-x}Cu_2O_{8+y}$ system.

		Pr				Gd				Er			
	Comp.x	0.50	0.6	0.5	0.6	0.8		0.97		0.5	0.6	0.97	
T	T_0 ($\times 10^3$) K[a]	0.28	6.0	0.78	25	1440	35	1200	748	0.7	37	370	45
(K)	a (Å)[b]	57	20	42	13	3	11	3.5	4	42.5	11	5	10
14	R (Å)[c]	50.5	39	46	35		33		26	47	33		33
	W (mev)[d]	0.55	1.2	0.07	1.65		2		4.0	0.7	2.0		1.98
20	R (Å)	46	36	42	32		31		23	43	23		30
	W (mev)	0.07	14.5	0.96	2.2		2.4		5.9	0.9	5.85		2.64
60	R (Å)	35	27	32	24	17		17		32.6	21	19.0	
	W (mev)	1.66	3.6	2.2	5.2	14.5		14.5		2.0	7.7	10.0	
100	R (Å)	31	24	28	21	15		15		28.7	19	17	
	W (mev)	2.4	5.2	3.2	7.7	21		21		3.0	10	14.5	
150	R (Å)	28	22	25	19	13		14		26	17	15.0	
	W (mev)	3.2	6.7	4.5	10	32		26		4.0	14.5	21.0	
200	R (Å)	26	20	24	18	12		13		24.0		14	
	W (mev)	4.0	9.0	5.2	12	41		32		5.15		26	
250	R (Å)	25	19	23	17	11.5		12		23		13.0	
	W (mev)	4.5	10.0	5.8	14.5	47		41		5.8		32	
300	R (Å)	23.5	18	22	16	53.5		11.5		22		12.5	
	W (mev)	5.5	12	6.7	17	11		47		6.7		36	

[a]The characteristic temperature T_0 calculated from the equation $\rho=\rho_0\exp(T_0/T)^{1/4}$.
[b]The localization length α (exponential decay of the electronic wave function at large distances) evaluated from Eq. (2).
[c]The hop distance or range R (distance between the initial and final states) calculated from Eq. (4).
[d]Activation energy (W) for a hop between two sites calculated from Eq. (5).

cess. Thus, the electron reaches the final state by this indirect or exchange transition. The hopping length (R) is independent of the energy difference between the two states and can be large even for very small values of W. The values of T_0 obtained directly from the slopes of the plots Fig. 7 range from 10^2–10^6 K. An increase in T_0 implies a decrease in either the localization length or density of states at E_F. We have assumed a constant value for $N(E_F)$ ($\sim$3.03 states/ev-cell) (Ref. 38) since band structure calculations have shown that the Fermi level lies in a broad peak (rigid band) of almost constant density of states. Therefore, we do not expect a drastic change in $N(E_F)$ with change in rare-earth concentration and any change in $N(E_F)$, should lie within error bars. Similar studies have been made on other systems[39] assuming a constant value of density of states at E_F.

It is known that high T_0 value is an indication of multiphonon hopping and our results show that T_0 values are large for higher concentrations (x=0.8 and 0.97) as compared to that for x=0.5 and 0.6. The localization lengths are evaluated using Eq. (2) (Table I). It is interesting to note that as the dopant concentration increases, the T_0 values increase and the localization lengths decrease in a systematic way. For a hop to take place, the initial state must be occupied and the final state empty, so that the tunneling transitions are restricted to a region very close to the Fermi energy. Within this narrow range, $N(E_F)$ and the localization length remain constant as a function of temperature. At any temperature, the transition probability[40] for the occurrence of a hop to a state at a distance R from the initial state and separated by an energy W, is given by

$$p \sim \exp[-2\alpha R - (W/kT)] . \quad (3)$$

The term $\exp(-2\alpha R)$ denotes the probability of finding an electron at a distance R from its initial state and α is the inverse localization length (a) as explained earlier. Since the hopping takes place by tunneling between two states, α remains almost a constant within the range where the VRH is satisfied except when there is a change in slope (x=0.8 of Gd and 0.97 of Gd and Er) at low temperatures. The hop distance (R) varies with temperature and hence the term "variable range hopping" is used to describe the conduction mechanism. The value of R is calculated using the relation

$$R = [3a/2\pi N(E_F)kT]^{1/4} . \quad (4)$$

The second term in Eq. (3), expressed by the Boltzmann factor, $\exp(-W/kT)$ arises due to the phonon assistance required by the electron in overcoming the energy barrier W. At high temperatures, the electrons gain sufficient energy to hop to neighboring states (small values of R) with large values of W. At any given temperature, electrons normally jump to sites for which the activation energy, W is as low as possible. Because of the second term in Eq. (3), the hopping probability p, decreases with decreasing temperature which implies that, it becomes more difficult for an electron to overcome a given energy barrier W. The electron, therefore, prefers to hop to sites with lower values of W. Thus, at low temperatures, the probability may be enhanced by permitting the electron to jump to sites within a larger neighborhood of radius R surrounding the initial site and for this site,

$$W = 3/4\pi R^3 N(E_F) . \quad (5)$$

The combination of R and W is such that only the most dominant hops contribute to the conductivity at any temperature. The parameters R and W were calculated from Eqs. (4) and (5), respectively in the range 20–300 K and are listed in Table I. A typical variation of R and W as a function of temperature is shown in the inset of Fig. 7. As can be seen, W decreases systematically and R also increases with decrease in temperature which corroborates well with the Mott's hypothesis of VRH mechanism. For higher dopant concentrations (0.8 and 0.97) in the Bi-2212 system, the condition that $R \gg \alpha$ and $W \gg kT$ holds good which shows that the materials which are on the metallic side of the Mott transition are subjected to increasing disorder and the highly disordered materials (x=0.8 and 0.97) satisfy all the Anderson's localization conditions (small localization length and large hopping length etc.) that lead to the Mott's VRH behavior. Also it is evident from Fig. 7 that the $\ln\rho - (1/T^{1/4})$ behavior for x = 0.5–0.97 excellently matches with the expected behavior.[28,41] The phonon frequencies calculated using the formula

$$\nu_{ph} = 2(8\pi)^{1/2}/e^2\sigma_0[N(E_F a/kT)]^{-1/2}$$

are in the range 10^{10}–10^{12} s^{-1} which is within the expected range.[28,29,32]

CONCLUSIONS

Systematic electrical resistivity and magnetic susceptibility studies carried out on the $Bi_{2.1}Sr_{1.93}(Ca_{0.97-x}R_x)Cu_2O_{8+y}$ (R=Pr, Gd, Er) system have indicated that the T_c systematically decreases with increase in the rare-earth ion concentration at the Ca site. However, the rate of T_c suppression is independent of the size and magnetic nature of the substituent ions and is observed to follow the same trend in all the three rare-earth doped phases. This clearly indicates that the Pr ion has no additional effect on the T_c suppression unlike in the Pr-doped Y-123 system. We have shown that hole filling, rather than AG magnetic pair breaking is responsible for the T_c suppression. The phases with $x \geq 0.5$ show a semiconducting behavior and satisfy the Mott's variable range hopping mechanism for electronic conduction. The increase in disorder in the materials is evident at high dopant concentrations. The calculated values of R and W show a systematic trend obeying Mott's postulates.

ACKNOWLEDGMENT

P.S.P. wishes to thank the NSTB-DST, New Delhi for financial support.

[1]A. Kebede, C. S. Jee, D. Nichols, M. V. Kuric, J. E. Crow, R. P. Guertin, T. Mihalisin, G. H. Myer, I. Perez, R. E. Salomon, and R. Schlottmann, J. Magn. Magn. Mater. **76&77**, 619 (1988).

[2]T. Tamegai, K. Koga, K. Suzuki, M. Ichihara, F. Sakai, and Y. Iye, Jpn. J. Appl. Phys. **28**, L112 (1989).

[3]D. Mandrus, L. Forro, C. Kendziora, and L. Mihaly, Phys. Rev. B **44**, 2418 (1991).

[4]Y. Gao, P. Pernambuco-Wise, J. E. Crow, J. O'Reilly, N. Spencer, H. Chen, and R. E. Salomon, Phys. Rev. B **45**, 7436 (1992).

[5]A. Maeda, M. Hase, I. Tsukada, K. Noda, S. Takebayashi, and K. Uchinokura, Phys. Rev. B **41**, 6418 (1990).

[6]A. Manthiram and J. B. Goodenough, Appl. Phys. Lett. **53**, 2695 (1988).

[7]A. A. Abrikosov and L. P. Gor'kov, Sov. Phys. JETP **12**, 1243 (1961).

[8]T. Ishida, Jpn. J. Appl. Phys. **27**, L2327 (1988).

[9]T. Ishida and T. Sakuma, Jpn. J. Appl. Phys. **27**, L1237 (1988).

[10]A. K. Sarkar and I. Maartense, Physica C **168**, 591 (1990).

[11]T. Ishida, K. Koga, S. Nakamura, Y. Iye, K. Kanoda, O. Okui, T. Takahashi, T. Oashi, and K. Kumagai, Physica C **176**, 24 (1991).

[12]D. P. Almond, B. Chapman, and G. A. Sounders, Supercond. Sci. Technol. **1**, 123 (1988).

[13]C. Namgung, J. T. S. Irvine, J. H. Binks, E. E. Lachowski, and A. R. West, Supercond. Sci. Technol. **2**, 181 (1989).

[14]A. Ono, Jpn. J. Appl. Phys. **28**, L1372 (1989).

[15]V. P. S. Awana, S. K. Agarwal, A. V. Narlikar, and M. P. Das, Phys. Rev. B **48**, 1211 (1993).

[16]A. Manthiram and J. B. Goodenough, Appl. Phys. Lett. **53**, 420 (1988).

[17]B. Jayaram, P. C. Lanchester, and M. T. Weller, Physica C **160**, 17 (1989).

[18]Y. Y. Xue, P. H. Hor, Y. Y. Sun, Z. J. Huang, L. Gao, R. L. Meng, C. W. Chu, J. C. Ho, and C. W. Wu, Physica C **158**, 211 (1989).

[19]J. M. Tarascon, P. Barboux, G. W. Hull, R. Ramesh, L. H. Greene, M. Girond, M. S. Hegde, and W. R. McKinnon, Phys. Rev. B **39**, 4316 (1989).

[20]S. Olivier, W. A. Groen, C. van der Beek, and H. W. Zandbergen, Physica C **157**, 531 (1989).

[21]K. Koyama, S. Kanno, and S. Noguchi, Jpn. J. Appl. Phys. **28**, 1354 (1989).

[22]S. B. Samanta, P. K. Dutta, V. P. S. Awana, E. Gmelin, and A. V. Narlikar, Physica C **178**, 171 (1991).

[23]R. B. Goldfarb, M. Lenenthal, and C. A. Thompson (unpublished).

[24]P. Sumana Prabhu, M. S. Ramachandra Rao, and G. V. Subba Rao, Physica C **211**, 279 (1993).

[25]C. S. Gopinath, S. Subramanian, P. Sumana Prabhu, M. S. Ramachandra Rao, and G. V. Subba Rao, Physica C **218**, 117 (1993).

[26]M. Tinkham, *Introduction to Superconductivity* (McGraw Hill, New York, 1975).

[27]S. Sugai and M. Sato, Jpn. J. Appl. Phys. **28**, L1361 (1989).

[28]N. F. Mott and E. A. Davis, *Electronic Processes in Non-Crystalline Materials* (Clarendon, Oxford, 1979).

[29]P. Nagel, in *Topics in Applied Physics,* edited by M. H. Brodsky (Springer, Berlin, 1979), Vol. 36, p. 113.

[30]M. A. Kastner, R. J. Birgeneau, C. Y. Chen, Y. M. Chiang, D. R. Gabbe, H. P. Jenssen, T. Junk, C. J. Peters, P. J. Picone, T. Thio, T. R. Thurston, and H. L. Tuller, Phys. Rev. B **37**, 111 (1988).

[31]K. Sreedhar and P. Ganguly, Phys. Rev. B **41**, 371 (1990).

[32]Paracchini, G. Calestani, and M. G. Francesconi, Physica C **167**, 249 (1990).

[33]R. K. Nkum and W. R. Datars, Phys. Rev. B **46**, 5686 (1992).

[34]B. Jayaram, P. C. Lanchester, and M. T. Weller, Phys. Rev. B **43**, 10 589 (1991).

[35]D. Emin, in *Electronic and Structural Properties of Amorphous Semiconductors,* edited by P. G. Le Comber and J. Mort (Academic, London, 1973), p. 261.

[36]D. Emin, Phys. Rev. Lett. **32**, 303 (1974).

[37]M. L. Knotek and M. Pollak, Phys. Rev. B **9**, 664 (1974).

[38]S. Massidda, J. Yu, and A. J. Freeman, Physica C **152**, 251 (1988).

[39]Wu Jiang, J. L. Peng, J. J. Hamilton, and R. L. Greene, Phys. Rev. B **49**, 690 (1994), and Ref. 5 therein.

[40]R. Zallen, *Physics of Amorphous Solids* (Wiley, New York, 1983).

[41]N. F. Mott, M. Pepper, S. Pollitt, R. H. Wallis, and J. Adkins, Proc. R. Soc. London Ser. A **345**, 169 (1975).